

Experimental study about the influence of Wire EDM parameters on surface roughness and kerf width of Ti-3Al-2.5V superalloy

H. Mohamed Suhail^{1*}, Nandakumar Chinnamuthu¹, Senthilkumar Chinnamuthu²

¹*Department of Production Technology, Madras Institute of Technology, Anna University, Chromepet, Chennai – 600 044, Tamil Nadu, India*

²*Department of Mechanical Engineering, University College of Engineering (Panruti), Anna University, Panruti – 607 106, Tamil Nadu, India*

Received 4 June 2024, received in revised form 11 June 2024, accepted 20 June 2024

Abstract

Ti-3Al-2.5V superalloy is a highly structural and functional material predominantly used in hydraulic tubing for aircraft like Boeing and honeycomb structures in structural applications. In this study, the Wire Electrical Discharge Machining input parameters considered for observation were Pulse on time (T_{on}), Pulse off time (T_{off}), Wire Feed (WF), and Wire Tension (WT). The output responses analyzed were kerf width (KW) and Surface Roughness (SR). Taguchi's L_{16} orthogonal array was used for conducting experiments. The smallest and largest kerf width values observed were 0.311 and 0.344 mm, respectively. The lowest and highest surface roughness values observed were 1.530 and 2.649 μm , respectively. Signal-to-noise ratio response and Analysis of Variance revealed that Pulse on time (T_{on}) was the most influential parameter affecting kerf width and surface roughness. Microstructure analysis of machined samples and wire electrodes was carried out with a Scanning Electron Microscope.

Key words: surface roughness, scanning electron microscopy, surface characterization, titanium-based superalloy, Wire EDM, kerf width

1. Introduction

Titanium and its alloys have significantly impacted today's aerospace, automotive, and biomedical industries [1, 2, 5]. These alloys also have applications in food processing, shipbuilding, and chemical engineering [3]. However, the question that intrigues our mind is what makes this group of alloys desirable in these domains. Some of the crucial reasons could be their phenomenal strength-to-weight ratio, exceptional corrosion resistance, high heat transfer efficiency, and brilliant erosion resistance, to name a few [2]. Currently, a wide variety of titanium alloys are available on the market. However, we can categorize them into three chief groups as α alloys, β alloys, and $\alpha + \beta$ alloys, based on the alloying elements used [1]. Generally, in pure titanium, the α phase (hexagonal close-packed structure) is stable up to a temperature of 1153 K. However, beyond this temperature, it transforms into a body-centered cubic structure known as

β phase, and this temperature is called as β transition temperature [2]. Based on the effect induced by the alloying elements in pure titanium, we can classify them as α stabilizers and β stabilizers. The addition of α stabilizers increases the β transition temperature, as mentioned before. Conversely, the addition of β stabilizers reduces this transition temperature [1, 2]. Some common examples of α stabilizers are aluminum (Al) and tin (Sn). On the other hand, alloying elements like vanadium (V), molybdenum (Mo), chromium (Cr), and copper (Cu) are examples of β stabilizers [2].

Now that we have discussed the desirable properties, application domains, and classification of titanium alloys, the next question that pops into our minds is the machinability aspect of these alloys. Generally, nickel-based alloys and titanium-based alloys are regarded as highly difficult-to-machine materials [5]. In general, machining difficult-to-machine materials like these titanium alloys using conventional or

*Corresponding author: e-mail addresses: suhailhjv@gmail.com; suhail@mitindia.edu

traditional machining methods is costly [4]. The main drawbacks of implementing conventional machining include high tool wear, poor surface finish, prolonged machining time, and inability to accomplish some intricate or complex shapes [4, 6]. To overcome these drawbacks, we can implement non-conventional machining techniques like Laser Beam Machining (LBM), Water Jet Machining (WJM), Electro Discharge Machining (EDM), Wire Electrical Discharge Machining (WEDM), etc. [6]. Among these non-conventional techniques, EDM is used widely due to its ability to machine difficult-to-machine materials in different complex shapes [4].

Wire Electrical Discharge Machining is an unconventional method that electrically eliminates material from any conductive workpiece, irrespective of its hardness [7]. When a metallic wire performs as a tool electrode in the EDM process, it is referred to as Wire Electrical Discharge Machining, and its operation is like that of cutting using a band saw [4]. The basic principle of WEDM is the melting and evaporation of material from the workpiece with the assistance of a wire, which is subjected to direct current in the presence of an insulating dielectric medium [7]. The following literature review will explore some of the different alloys machined via WEDM and the respective wire electrodes researchers implemented recently.

Basavaraju et al. have investigated the effect of process parameters like Pulse-on time (T_{on}), Pulse-off time (T_{off}), and Indicated Power (IP) on the Surface roughness (Ra) and Material Removal Rate (MRR) for Grade 7 Titanium alloy, which was machined using WEDM. The wire electrode used here was a zinc (Zn) coated brass wire with a diameter of 0.25 mm. Additionally, the researchers have employed an L_{27} orthogonal array as their Design of Experiment (DOE). Based on the results obtained from the statistical techniques, it was found that T_{on} and peak current greatly impacted MRR. Moreover, the most significant factor that had an impact on MRR and Ra was found to be T_{off} at 58.81 and 36.11 %, respectively. Another point to be noted was that the MRR decreased as the T_{off} increased because of the reduced spark discharges during this period. The high discharge energy produced due to increased peak current affected the surface finish significantly [8].

Veere et al. optimized the process parameters for machining Ti-16Al-14Nb (α/β , ML-Grade) alloy using Wire Electrical Discharge Machining. The selected process parameters were Pulse on duration, Peak current, and Pulse off duration. The design of experiments was based on a 3×3 factorial design. Kerf width, MRR, and surface roughness were the selected performance measures in this research. High MRR and surface roughness were observed at the maximum level of input factors. ANOVA results showed that peak current and pulse-on duration significantly influenced

the performance measures compared to pulse-off duration. The authors concluded by identifying the desirability of optimal solutions [9].

Ezeddini et al. investigated the impact of WEDM process parameters such as feed rate, servo voltage, pulse on duration, and flushing pressure on surface finish during machining of the Ti-6242 superalloy. The machining of this alloy was carried out using a brass wire electrode. The DOE was based on Taguchi's L_9 orthogonal array. This study exposed that reducing pulse on duration and feed rate at high servo-voltage led to minimal surface damage caused by machining. Similarly, it was found that surface micro-crack density was influenced by pulse on duration at greater levels of feed rate and servo voltage [10].

Mussada has modeled and predicted the process parameters for machining Grade 2 Titanium alloy using WEDM. Six input parameters, such as peak current (I_p), T_{on} , servo feed, servo voltage, wire tension, and wire feed, were chosen for this study. Material Removal Rate (MRR) and Power consumption (P_c) were considered as output responses. This study adopted an Adaptive Neuro Fuzzy Interface System (ANFIS) to construct the predictive models for the output mentioned above responses. Based on the conclusions drawn, it was evident that MRR increased significantly with an increase in pulse on time and peak current [11].

Satyanarayana et al. have conducted experimental studies on Inconel 600 machined in WEDM. Zinc-coated wire has been used to machine this nickel-based alloy. Nine experiments were carried out in this study. Input current, T_{on} , and T_{off} were the selected machining parameters. In this study also, the selected output responses were MRR and Ra . ANOVA analysis revealed that Pulse on time had the most significant impact on surface roughness at 35.59 %, and current had the most significant impact on MRR at 70.74 %. The optimization results exposed that MRR was optimum at current – 8 A, pulse on – 4 μ s, and pulse off – 5 μ s. Similarly, the Ra was optimum at current – 4 A, pulse on – 2 μ s, and pulse off – 9 μ s [12].

Prasana et al. have optimized the WEDM machining parameters for α -phase Ti 6242 alloy. A brass wire of diameter 0.25 mm was used for machining. This study considered four machining parameters: T_{on} , T_{off} , voltage, and wire feed rate. The adopted DOE was Taguchi's L_{27} orthogonal array. The Technique for Order of Preference by Similarity to Ideal Solution (TOPSIS) methodology has been implemented in this research to perform optimization. Based on the results obtained from this TOPSIS methodology, high MRR, and good surface finish were achievable at pulse on time of 6 μ s, pulse off time of 6 μ s, voltage of 80 V, and wire feed rate of 4 m min^{-1} [13].

Aggarwal et al. executed the empirical modeling of WEDM process parameters for machining Inconel 690

superalloy. The modeling has been done via Response Surface Methodology (RSM) with input parameters such as T_{on} , T_{off} , peak current, and spark voltage. This research considers surface roughness and cutting rate as output responses. A zinc-coated brass wire with a 0.25 mm diameter has been used as the electrode for machining Inconel 690. The central composite design (CCD) has been applied as the DOE in this study. The conclusive results showed that T_{on} had the most prominent impact on cutting rate and surface finish [14].

Kumar et al. used Grade 5 Titanium alloy (Ti-6Al-4V) as the workpiece to conduct their study. The machining was carried out using a brass wire of 0.25 mm diameter. Taguchi's L_{18} orthogonal array was utilized for conducting experiments. The input parameters considered for experiments were T_{on} , T_{off} , peak current, and servo voltage. In addition, MRR, surface roughness, and kerf width were selected as output responses in this study. Once the experiments were carried out, optimization was done using the Grey Relational Analysis methodology. The results revealed that 100 μ s – pulse on time, 50 μ s – pulse off time, 12 A – peak current, and 10 V – servo voltage was the optimal combination of process parameters [15].

Majumder & Maity have implemented a General Regression Neural Network (GRNN) and Multiple Regression Analysis (MRA) to perform predictive analysis. In this experimental study, Grade 6 Titanium alloy was machined using brass wire. The selected machining parameters were T_{on} , T_{off} , wire feed, and wire tension. The experiments were carried out based on Taguchi's L_{27} orthogonal array. The output responses considered were surface roughness, MRR, and kerf width. The results concluded that the GRNN model displayed lesser estimated error than the MRA model [16].

Kumar et al. implemented an integrated Genetic Algorithm (GA) approach with Response Surface Methodology (RSM) to optimize WEDM process parameters. Nimonic-90, a nickel-based superalloy, has been employed as the work material in this research work, and the corresponding wire electrode used to machine it was zinc-coated brass wire. Servo voltage, discharge current, T_{on} , and T_{off} were selected as the input parameters. Since the RSM methodology was utilized, the DOE was based on Central Composite Design (CCD). The only output response considered in this study was surface roughness. The obtained results showed that T_{on} had the most substantial impact on surface roughness [17].

Reolon et al. have compared the performance of coated and uncoated wires while machining IN718 alloy using WEDM. Uncoated and zinc-coated brass wires have been used for this comparative study. The input parameters selected in this research were pulse interval duration, wire speed, and discharge period.

The output characteristics analyzed were kerf width, recast layer, and wire feed. Implementing optimized WEDM process parameters exposed a significant increase in wire feed rate for zinc-coated and uncoated wires at 35 and 36 %, respectively. Similarly, for the optimized condition, there was a prominent reduction in wire consumption for zinc-coated and uncoated wires at 40 and 80 %, respectively [18].

Prathik et al. studied the Acoustic Emission (AE) signals and surface roughness characteristics for Grade 2 Titanium alloy machined using WEDM. For machining purposes, a molybdenum wire with a diameter of 0.18 mm has been utilized in this experimental investigation. Model development and estimation have been done with the help of Artificial Neural Network (ANN). The process parameters varied in this study were current, bed speed, pulse on time and pulse off time. In addition, experiments were performed based on Taguchi's L_{16} orthogonal array. Conclusive results showed an increase in roughness plot at maximum cutting condition. Moreover, it was found that training the neural network with 70 % of data in the training set unveiled better results than 50 or 60 % of data in the training set [19].

Shri & Rahul have conducted an experimental investigation in machining cold-pressed Grade 2 Titanium alloy using WEDM. The machining was carried out using a 0.25 mm diameter brass wire. This study uses seven variable parameters: wire feed rate, wire tension, servo feed rate, flushing pressure, peak current, pulse on time, and pulse off time. The experiments have been designed based on Taguchi's L_{27} orthogonal array. Additionally, a brass wire with a 0.25 mm diameter has been utilized as the wire electrode for machining this alloy. This research focused on minimizing surface roughness by optimizing the input parameters [20].

Saedon et al. have investigated the effect of input process parameters such as peak current, wire feed, pulse-off time, and wire tension on the machinability aspects like material removal rate, cutting rate, kerf width, and surface roughness during the machining of Grade 5 Titanium alloy in WEDM. Optimization was done using Grey Relational Analysis (GRA) and Analysis of Variance (ANOVA). The results of this study exhibited that noteworthy improvement in machining performance was attainable with this optimization method [21].

Nandakumar & Mohan have performed multi-objective optimization for machining Ti-6Al-4V alloy using WEDM. The technique that they have implemented for performing optimization is Response Surface Methodology (RSM). This research aimed to optimize input parameters like pulse on time, pulse off time, and wire feed rate to attain high MRR and good surface finish. After experimentation, conclusions were drawn that surface roughness and material removal

rate were amplified with an increase in pulse on time. In addition, pulse off time seemed to have a meager effect on surface roughness compared to other parameters [22].

The literature review revealed that Grade 5 Titanium alloy and nickel-chrome-based superalloys had been widely used for experimental investigations related to Wire Electrical Discharge machining. The commonly implemented wire electrodes were either plain brass wire electrode (or) zinc-coated wire electrode. The extensive literature review revealed that experimental studies of Grade 9 Titanium alloy concerning WEDM is a lesser explored area and is the primary research gap that led to this experimental study. Additionally, using special wire electrodes like diffusion annealed wire to machine the alloy mentioned above is not very common, which is another identified research gap from the literature. In this regard, we will observe the influence of process parameters on kerf width and surface roughness obtained during the machining of Grade 9 Titanium alloy using diffusion-annealed wire electrode. This study will give a clear understanding of the impact of Wire EDM input process parameters on critical output responses such as kerf width and surface roughness during machining of Ti-3Al-2.5V alloy. The alloy used in this study, i.e., Ti-3Al-2.5V alloy, finds applications primarily in honeycomb structures and aircraft tubings. So, the findings of this study will contribute to manufacturing engineers in these sectors as it will give them an overview of what input process parameters to monitor during the machining of this alloy in Wire EDM. This, in turn, will help them achieve defect-free components with good surface finish that are dimensionally accurate.

2. Materials and methods

2.1. Material

Grade 9 Titanium alloy (Ti-3Al-2.5V) with dimensions of $200 \times 200 \times 10 \text{ mm}^3$ has been considered the workpiece in this study. The chemical composition of this alloy is shown in Table 1 [23]. This alloy is primarily used in hydraulic high-pressure lines. Replacing the stainless-steel pipes with this alloy in these hydraulic high-pressure lines can reduce weight by 40 % [3].

Ti-3Al-2.5V alloy also finds application in the manufacture of honeycomb structures, which provides improved strength compared to honeycomb structures made of cold-pressed titanium [1].

2.2. Design of Experiments (DOE)

To analyze the relationship between input process parameters and output responses, we need to plan the

Table 1. Chemical composition of Grade 9 Titanium alloy

| Al | V | Fe | O | C | N | H | Ti |
|-----|-----|------|------|------|------|-------|---------|
| 3.2 | 2.5 | 0.25 | 0.12 | 0.05 | 0.02 | 0.012 | Balance |

Table 2. Levels of selected machining parameters

| Parameters | Level 1 | Level 2 | Level 3 | Level 4 |
|-----------------------------------|---------|---------|---------|---------|
| Pulse on time (μs) | 3 | 5 | 7 | 9 |
| Pulse off time (μs) | 8 | 10 | 12 | 14 |
| Wire Feed (m min^{-1}) | 2 | 4 | 6 | 8 |
| Wire Tension (grams) | 400 | 600 | 800 | 1000 |

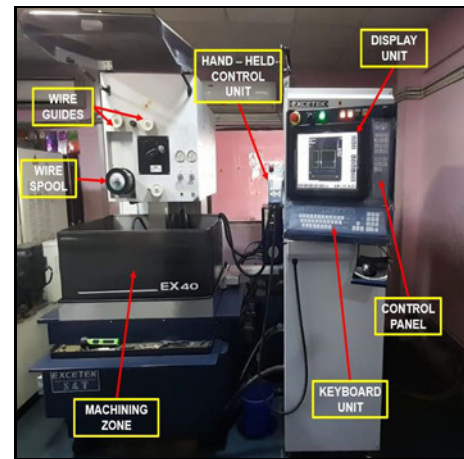


Fig. 1. EXCETEK – EX 40 WEDM setup.

experiments systematically. The procedure for planning these experiments in an efficient way is known as the Design of Experiments (DOE). The initial steps in creating a DOE are fixing the objective of the experiments and choosing the suitable process variables [24]. In our study, the objective is to observe the kerf width and surface roughness based on which they have been selected as output responses. Similarly, the selected input parameters for this study were Pulse on time, Pulse off time, wire tension, and wire feed. Table 2 shows the input parameters and their fixed levels based on literature review, pilot experiments, and machine constraints. Taguchi's L_{16} orthogonal array has been used as the DOE to conduct experiments.

2.3. Experimental setup

The machining of Ti3Al2.5V alloy was done using an EXCETEK-EX 40-wire electrical discharge machine, as shown in Fig. 1. D-type diffusion annealed

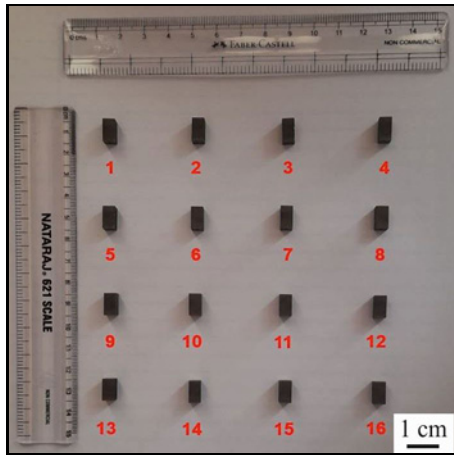


Fig. 2. Machined samples.

wire with a diameter of 0.25 mm has been used for machining in this study. This type of wire has a brass core surrounded by a special beta-phase coating, significantly improving mechanical and breaking strength [25]. Deionized water was used as the dielectric fluid. The dimensions of the machined samples were $5 \times 5 \times 10 \text{ mm}^3$. Figure 2 shows the machined samples.

2.4. Measurement of output responses

2.4.1. Surface roughness

Surface roughness is a crucial aspect when it comes to the tribological function of any component. Surface roughness also significantly affects mechanical properties like fatigue behavior, corrosion resistance, and creep life [26]. Added to this, surface roughness also plays a key role in defining the functionality of a product [27]. In this study, the surface roughness of the samples was measured using the MarSurf PS 10 apparatus, as shown in Fig. 3. It is a contact-based stylus instrument used for surface measurements. Initially, the specimen is held in place by clamping it using a bench vice, as shown in Fig. 4a. Next, the stylus tip is placed perpendicular to the surface to be measured, as shown in Fig. 4b. The surface roughness measurements were carried out with an evaluation length of 4 mm and a cut-off length of 0.8 mm as per standard practice [28]. Three readings were taken for each specimen, and their average was noted.

2.4.2. Kerf width

One of the critical performance measures in WEDM is kerf. The reason for this is that the dimensional accuracy of the finished component depends on this kerf [29]. In simple terms, kerf can be defined as the width

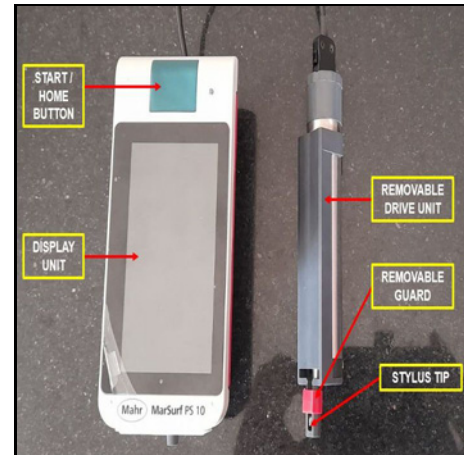


Fig. 3. Surface roughness measurement apparatus.

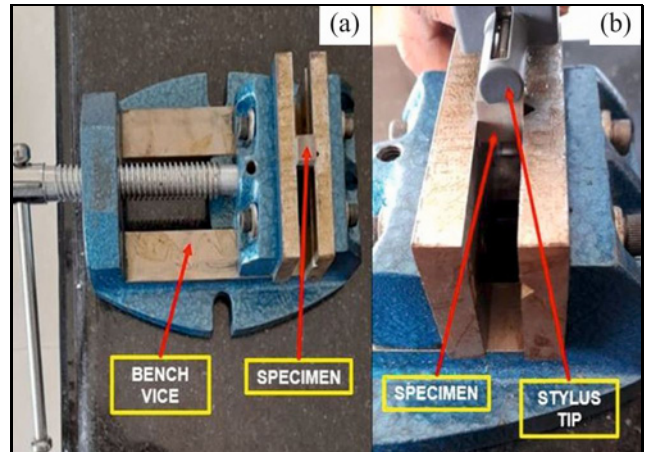


Fig. 4. (a) Clamping of the specimen and (b) position of the stylus tip.

of the cut for which the cut has been taken. Added to this, the kerf width is generally greater than the diameter of the wire electrode used for machining [30]. The kerf width was observed using a Celestron Capture Pro Stereo microscope, as shown in Fig. 5. It is equipped with a 5 MP camera to capture and save high-resolution images. Once the required image was captured, the kerf width was measured with the help of an image analysis software known as *Dewinter Material Plus* (Version 4.5). Three readings along the kerf channel were noted for each specimen at the top and bottom, respectively, and their average was recorded.

2.5. Taguchi method

Genichi Taguchi proposed the Taguchi method, which effectively studies an entire parameter space with fewer experiments. This method utilizes Signal-to-Noise ratios (S/N ratios) as a performance mea-

Table 3. Taguchi's L_{16} design of experiments and output responses

| Exp. No. | Input parameters | | | | Output responses | |
|----------|------------------------------------|--------------------------------------|--------------------------------|-------------------------|------------------|--|
| | Pulse on time T_{on} (μs) | Pulse off time T_{off} (μs) | Wire Feed WF ($m\ min^{-1}$) | Wire Tension WT (grams) | Kerf width (mm) | Average surface roughness Ra (μm) |
| 1 | 3 | 8 | 2 | 400 | 0.314 | 1.681 |
| 2 | 3 | 10 | 4 | 600 | 0.311 | 1.53 |
| 3 | 3 | 12 | 6 | 800 | 0.318 | 1.692 |
| 4 | 3 | 14 | 8 | 1000 | 0.316 | 1.929 |
| 5 | 5 | 8 | 4 | 800 | 0.325 | 1.948 |
| 6 | 5 | 10 | 2 | 1000 | 0.327 | 1.954 |
| 7 | 5 | 12 | 8 | 400 | 0.323 | 1.98 |
| 8 | 5 | 14 | 6 | 600 | 0.332 | 1.965 |
| 9 | 7 | 8 | 6 | 1000 | 0.332 | 2.158 |
| 10 | 7 | 10 | 8 | 800 | 0.335 | 2.288 |
| 11 | 7 | 12 | 2 | 600 | 0.335 | 2.306 |
| 12 | 7 | 14 | 4 | 400 | 0.333 | 2.261 |
| 13 | 9 | 8 | 8 | 600 | 0.342 | 2.649 |
| 14 | 9 | 10 | 6 | 400 | 0.331 | 2.522 |
| 15 | 9 | 12 | 4 | 1000 | 0.329 | 2.505 |
| 16 | 9 | 14 | 2 | 800 | 0.344 | 2.391 |

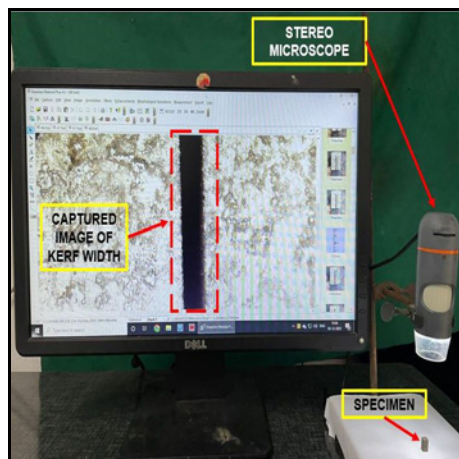


Fig. 5. Kerf width measurement setup.

sure [31]. In general, the purpose of the S/N ratio is to study the impact of noise factors on the desired output and minimize that effect [32].

In the Taguchi method, the term “signal” denotes the desirable nature (mean) of the output characteristic, and the term “noise” denotes the undesirable impact (or signal interference) of the output. This S/N ratio can help measure the sensitivity of the output response being monitored [33]. The quality characteristic can be categorized into three types: larger-the-better, smaller-the-better, and nominal-the-best [34].

The amount of material wastage occurring during machining in WEDM can be obtained from kerf [29]. Generally, higher kerf leads to higher material wastage. Keeping this in mind, we must try to

achieve minimal kerf during machining. Moreover, a smooth surface (lower surface roughness) is only preferred for most of the precision products that are manufactured [27]. Hence, in our study, we will choose “smaller-the-better” criteria for both kerf width and surface roughness [33]. The S/N ratios were calculated using Minitab 18 software.

3. Results and discussion

3.1. Influence of WEDM process parameters on the output responses

In this study, Taguchi's L_{16} orthogonal array was used to design the experiments using Minitab 18 software. The influence of process parameters was studied by utilizing the main effect plots generated using the S/N ratio. The measured output responses and the design of the experimentation are shown in Table 3.

3.1.1. Kerf width

Generally, WEDM is utilized to machine components with tight tolerances. The accuracy and precision of such components can be maintained by achieving smaller kerf widths during machining [35]. Kerf width also influences the internal corner radius generated by using WEDM [36]. Figure 6 shows the kerf width values for the sixteen experiments that were conducted.

Figure 6 shows that the minimal kerf width of 0.311 mm was obtained from experiment number 2 ($T_{on} = 3\ \mu s$, $T_{off} = 10\ \mu s$, $WF = 4\ m\ min^{-1}$, and

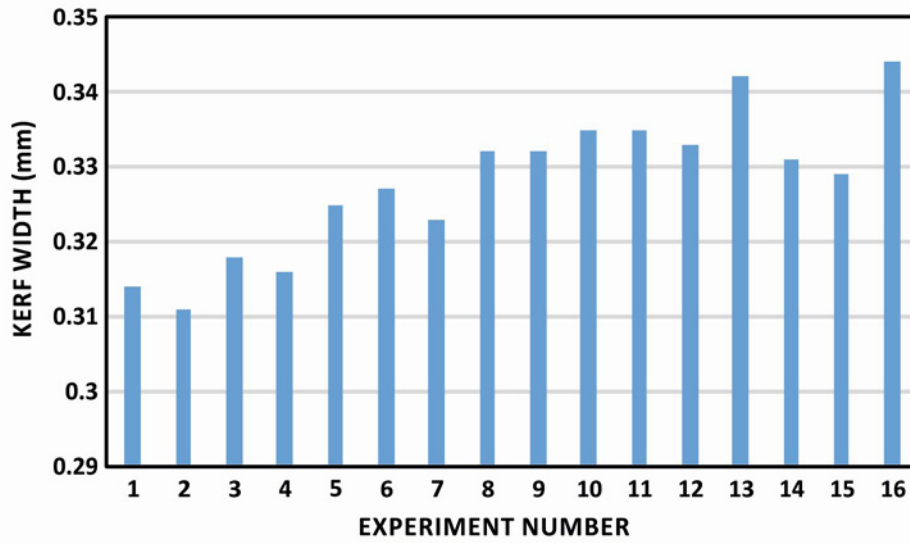


Fig. 6. Kerf width output.

Table 4. Response table of S/N ratio for kerf width (smaller-is-better)

| LEVEL | T_{on} (μs) | T_{off} (μs) | WF ($m\ min^{-1}$) | WT (grams) |
|-------|----------------------|-----------------------|----------------------|------------|
| 1 | 10.041 | 9.680 | 9.635 | 9.578 |
| 2 | 9.716 | 9.739 | 9.779 | 9.635 |
| 3 | 9.532 | 9.731 | 9.677 | 9.620 |
| 4 | 9.462 | 9.601 | 9.660 | 9.737 |
| DELTA | 0.579 | 0.138 | 0.144 | 0.138 |
| RANK | 1 | 3 | 2 | 4 |

WT = 600 grams). On the contrary, the maximum kerf width of 0.344 mm was observed in experiment number 16 ($T_{on} = 9\ \mu s$, $T_{off} = 14\ \mu s$, $WF = 2\ m\ min^{-1}$, and $WT = 800\ grams$).

Based on the S/N ratio, the influence of WEDM process parameters on kerf width is shown in Table 4. Kerf width is heavily influenced by T_{on} . The second most influential parameter was Wire feed (WF). Comparatively, T_{off} and WT seemed to have a less significant effect on kerf width. The main effects plot for kerf width is shown in Fig. 7.

From Fig. 7, we can observe that as Pulse on time increases, kerf width also increases simultaneously. This increase in kerf width is associated with the high discharge energy produced by increased Pulse on time [35]. Conversely, kerf width decreased with an increase in Pulse-off time up to a certain point. Generally, lower pulse intensity and pulse frequency at high pulse-off intervals lead to reduced kerf width [37].

Initially, there was a decrease in kerf width from the wire feed of 2 to 4 $m\ min^{-1}$. After 4 $m\ min^{-1}$, when the wire feed is increased, there is a gradual increase in kerf width. The increased flushing and decrease in wire vibration amplitude at the beginning could be the reason for this reduced kerf width. However, once the

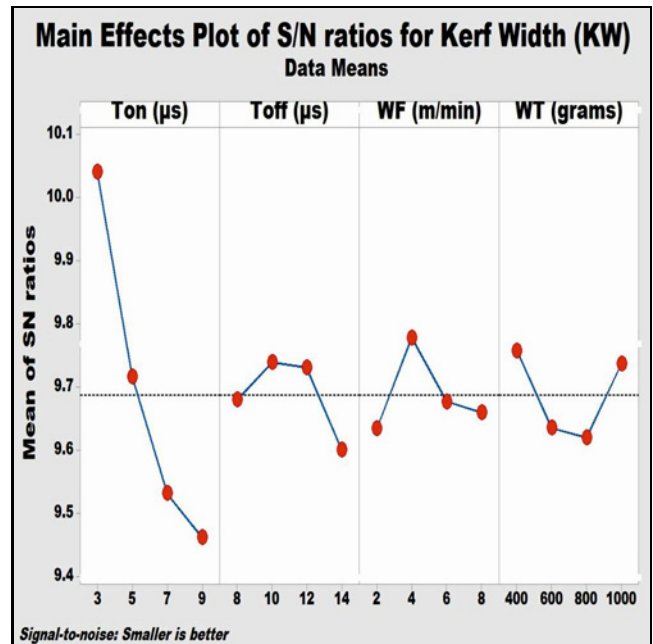
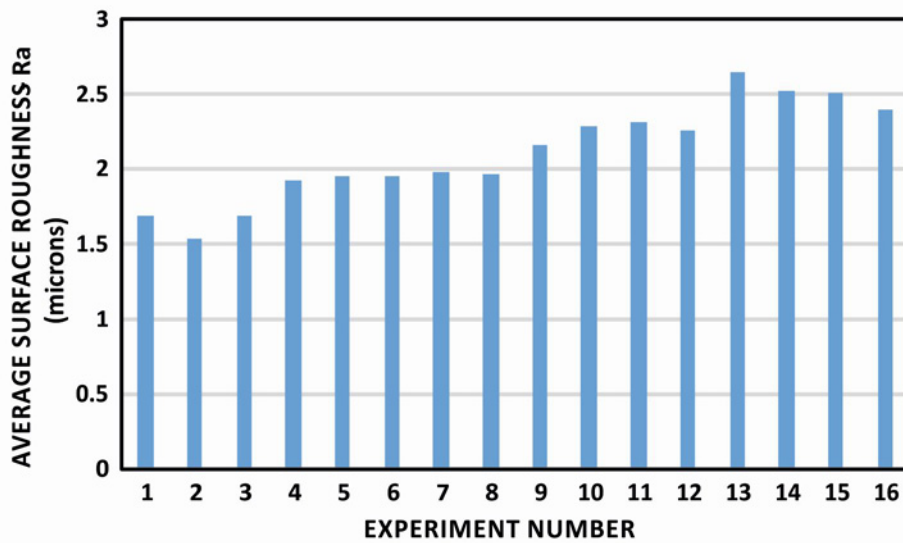


Fig. 7. Main effects plot of S/N ratios for kerf width.

Fig. 8. Average surface roughness (Ra) output.Table 5. Response table of S/N ratio for surface roughness (smaller-is-better)

| LEVEL | T_{on} (μs) | T_{off} (μs) | WF ($m\ min^{-1}$) | WT (grams) |
|-------|----------------------|-----------------------|----------------------|------------|
| 1 | -4.660 | -6.756 | -6.700 | -6.558 |
| 2 | -5.813 | -6.297 | -6.391 | -6.276 |
| 3 | -7.053 | -6.219 | -6.273 | -6.541 |
| 4 | -8.011 | -6.265 | -6.173 | -6.163 |
| DELTA | 3.351 | 0.537 | 0.527 | 0.395 |
| RANK | 1 | 2 | 3 | 4 |

wire feed reaches very high speeds, the destabilization of the wire causes an increase in kerf width [38].

The kerf width gradually increased in the lower wire tension range up to 800 grams. Once the wire tension was increased beyond this point, there was a reduction in kerf width. The wire remains stretchy, and its active length is longer at lower wire tensions (less than 800 grams in this study). This, in turn, increases generated heat, which leads to higher material removal and increased kerf width [39]. However, once the wire tension was increased further (greater than 800 grams in this study), it led to better wire straightness and decreased wire amplitude, contributing to the kerf width reduction [40].

3.1.2. Surface roughness

Evaluation of surface roughness is a critical aspect that holds the solution for many basic problems like positional accuracy, contact deformation, and friction. Surface finish is even considered a fingerprint for a machining process in the manufacturing sector [41]. Figure 8 shows the average surface roughness values (Ra) for the sixteen experiments that were conducted.

Figure 8 shows that the minimal average surface roughness of $1.530\ \mu m$ was obtained from experiment number 2 ($T_{on} = 3\ \mu s$, $T_{off} = 10\ \mu s$, $WF = 4\ m\ min^{-1}$, and $WT = 600\ grams$). The maximum average surface roughness of $2.649\ \mu m$ was observed in experiment number 13 ($T_{on} = 9\ \mu s$, $T_{off} = 8\ \mu s$, $WF = 8\ m\ min^{-1}$, and $WT = 600\ grams$).

Based on the S/N ratio, the influence of WEDM process parameters on surface roughness is shown in Table 5. The surface roughness of Ti-3Al-2.5V alloy is profoundly influenced by T_{on} . The second most influential parameter was found to be T_{off} . Comparatively, WF and WT seemed to have a lesser significant effect on surface roughness. The main effects plot for surface roughness is shown in Fig. 9.

From Fig. 9, it is evident that surface roughness increases with an increase in Pulse on time. The reason is that a shorter pulse on duration (3 and 5 μs in this study) will generate lesser discharge energy than a longer pulse on duration (7 and 9 μs in this study). Due to this lower discharge energy, shallow craters only form, which leads to smoother machined surfaces [39].

Regarding T_{off} , we can observe a declining trend

Table 6. ANOVA results for kerf width

| Source | DoE | Adj. SS | Adj. MS | F-value | P-value | Contribution (%) |
|----------------|-----|----------|----------|---------|---------|------------------|
| Pulse on time | 3 | 0.010653 | 0.003551 | 47.46 | 0.005 | 82.39 |
| Pulse off time | 3 | 0.000641 | 0.000214 | 2.85 | 0.206 | 4.96 |
| Wire feed | 3 | 0.000633 | 0.000211 | 2.82 | 0.209 | 4.90 |
| Wire tension | 3 | 0.000778 | 0.000259 | 3.47 | 0.167 | 6.02 |
| Error | 3 | 0.000224 | 0.000075 | – | – | 1.74 |
| Total | 15 | – | – | – | – | 100 |

R-sq. = 98.26 % R-sq. (adj.) = 91.32 %

Table 7. ANOVA results for surface roughness

| Source | DoE | Adj. SS | Adj. MS | F-value | P-value | Contribution (%) |
|----------------|-----|---------|---------|---------|---------|------------------|
| Pulse on time | 3 | 26.0970 | 8.6990 | 26.01 | 0.012 | 91.72 |
| Pulse off time | 3 | 0.5428 | 0.1809 | 0.54 | 0.687 | 1.91 |
| Wire feed | 3 | 0.4636 | 0.1545 | 0.46 | 0.729 | 1.63 |
| Wire tension | 3 | 0.3449 | 0.1150 | 0.34 | 0.798 | 1.21 |
| Error | 3 | 1.0034 | 0.3345 | – | – | 3.53 |
| Total | 15 | – | – | – | – | 100 |

R-sq. = 96.47 % R-sq. (adj.) = 82.37 %

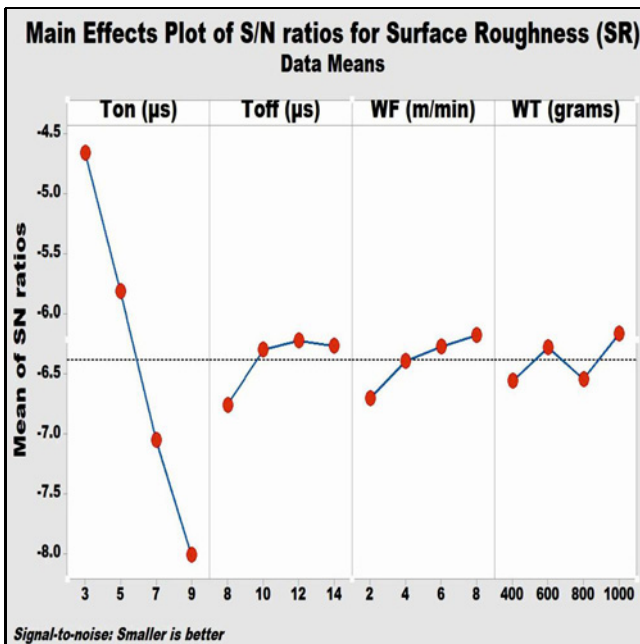


Fig. 9. Main effects plot of S/N ratios for average surface roughness (Ra).

in surface roughness with an increase in T_{off} . Very few discharges occur when the T_{off} duration is longer. This leads to a better surface finish due to the shallow nature of the craters produced during machining [42]. The surface roughness was found to decrease grad-

ually at higher wire feed rates. Similar results were observed by Rusdi Nur et al. [27].

When the wire tension was increased (above 800 grams in this study), surface roughness was considerably reduced. This could be because vibrations in the wire decrease with an increase in wire tension, which leads to smaller and shallower craters [43].

3.2. Analysis of Variance (ANOVA) for kerf width and surface roughness

The contribution or significance of each WEDM input process parameter to the output responses was determined in terms of percentage by utilizing ANOVA [44]. This contribution is represented by the F -value [45]. A 95 % confidence interval level was chosen to carry out this ANOVA analysis. To validate the significance or importance of an input process parameter in this 95 % confidence interval, the P -value must be less than 0.05 [44].

The ANOVA results for kerf width and surface roughness are shown in Table 6 and Table 7, respectively. These results revealed that Pulse on time had the lowest P -value and highest F -value in both cases, which shows that it is the most influential parameter affecting kerf width and surface roughness. The contribution of error was also minimal for kerf width and surface roughness, at 1.74 and 3.53 %, respectively. This shows that current data could be employed to estimate results in the future with a negligible degree of errors [44].

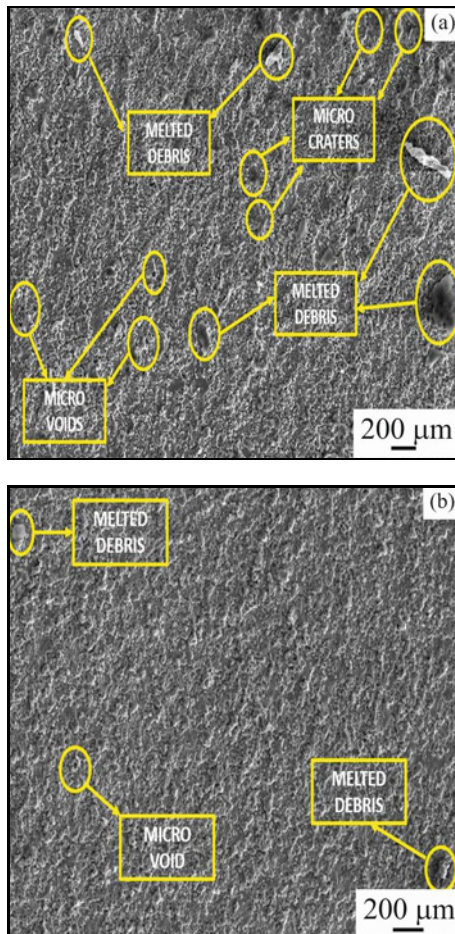


Fig. 10. (a) Microstructure of sample No. 13 ($T_{on} = 9 \mu s$, $T_{off} = 8 \mu s$, $WF = 8 \text{ m min}^{-1}$, $WT = 600 \text{ grams}$) and (b) microstructure of sample No. 2 ($T_{on} = 3 \mu s$, $T_{off} = 10 \mu s$, $WF = 4 \text{ m min}^{-1}$, $WT = 600 \text{ grams}$).

3.3. Surface analysis

The machined specimens with the highest and lowest surface roughness (Experiment number 13 and Experiment number 2, respectively) were examined using a Scanning Electron Microscope (SEM) to better understand their surface characteristics. The respective wire electrodes used for machining these specimens were also analyzed.

3.3.1. Machined specimens

Generally, the machined surfaces produced by WEDM are characterized by features like voids, craters, melted debris, cavities, and cracks [46], as shown in Figs. 10a, b.

Figure 10a shows that Sample number 13 has a rougher surface consisting of many surface defects compared to Sample number 2 in Fig. 10b, which seems to have a more uniform surface with negligible

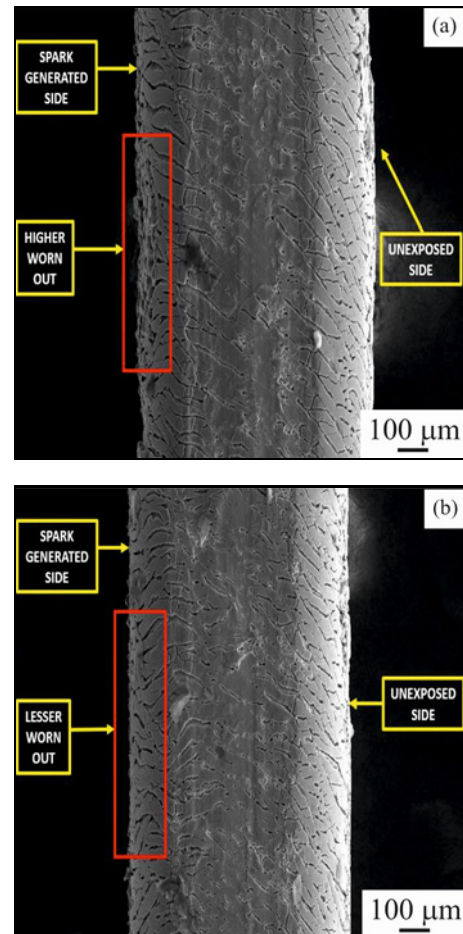


Fig. 11. (a) Microstructure of wire electrode used to machine sample No. 13 ($T_{on} = 9 \mu s$, $T_{off} = 8 \mu s$, $WF = 8 \text{ m min}^{-1}$, $WT = 600 \text{ grams}$) and (b) microstructure of wire electrode used to machine sample No. 2 ($T_{on} = 3 \mu s$, $T_{off} = 10 \mu s$, $WF = 4 \text{ m min}^{-1}$, $WT = 600 \text{ grams}$).

surface defects. This could be because the reduction of pulse on time (the most influential parameter for surface roughness in this study) leads to reduced heat generation. This, in turn, produces less debris, which can be easily flushed away from the machining zone. Hence, the machined surface is finer and more uniform [46].

3.3.2. Wire electrodes

Figures 11a,b show the SEM images of the corresponding wire electrodes used to machine Sample number 13 and Sample number 2.

From Figs. 11a,b, we can observe that the wire electrode subjected to moderate parametric settings (especially T_{on}) has a less worn-out area. The reason is that crater generation on the wire occurs at high voltage and current. The size of this crater is influenced by factors like Pulse on time and wire speed. Large-size craters on the wire surface (as shown in Fig. 11a)

lead to wire rupture and contribute to poor surface finish (Sample No. 13 has a Ra value of $2.649\ \mu\text{m}$ in this study) and poor machining accuracy [47].

4. Conclusions

Once the effect of WEDM process parameters on kerf width and surface roughness of Ti-3Al-2.5V alloy was studied and the corresponding microstructure analysis was carried out, the following conclusions were drawn:

1. The results indicate that Sample number 2 had the least kerf width of $0.311\ \text{mm}$, obtained with $T_{\text{on}} = 3\ \mu\text{s}$, $T_{\text{off}} = 10\ \mu\text{s}$, $\text{WF} = 4\ \text{m min}^{-1}$, and $\text{WT} = 600\ \text{grams}$.

2. On the contrary, the maximum kerf width of $0.344\ \text{mm}$ was observed in Sample number 16 while using the parametric combination of $T_{\text{on}} = 9\ \mu\text{s}$, $T_{\text{off}} = 14\ \mu\text{s}$, $\text{WF} = 8\ \text{m min}^{-1}$, and $\text{WT} = 800\ \text{grams}$.

3. An increase in kerf width was found to be associated with the high discharge energy produced by increased pulse on time. Conversely, lower pulse intensity and frequency at high pulse-off intervals lead to reduced kerf width.

4. Reduced kerf width was also observed for increased flushing and a decrease in wire vibration amplitude at the beginning of machining. However, once the wire feed reached very high speeds, the destabilization of the wire caused an increase in kerf width.

5. Improvement in wire tension led to better wire straightness and decreased wire amplitude, contributing to the reduction in kerf width.

6. Sample number 2 exhibited the lowest surface roughness of $1.530\ \mu\text{m}$, achieved with $T_{\text{on}} = 3\ \mu\text{s}$, $T_{\text{off}} = 10\ \mu\text{s}$, $\text{WF} = 4\ \text{m min}^{-1}$, and $\text{WT} = 600\ \text{grams}$.

7. The highest surface roughness of $2.649\ \mu\text{m}$ was detected in Sample number 13, which was subjected to $T_{\text{on}} = 9\ \mu\text{s}$, $T_{\text{off}} = 8\ \mu\text{s}$, $\text{WF} = 8\ \text{m min}^{-1}$, and $\text{WT} = 600\ \text{grams}$.

8. An increase in Pulse on time led to increased surface roughness due to the formation of deeper craters and other surface defects, which was also confirmed in SEM inspection of the machined surfaces.

9. Conversely, very few discharges were observed when the T_{off} duration was longer. This led to a better surface finish due to the shallow craters produced during machining, which was also confirmed by SEM inspection. Improvement in wire tension also led to reduced surface roughness.

10. The Signal-to-Noise ratio analysis (with ‘smaller-the-better’ criteria) revealed that T_{on} was the most influential process parameter that greatly impacted both kerf width and surface roughness, respectively. ANOVA also showed that T_{on} was the highest contributing factor affecting kerf width and surface roughness.

11. Surface analysis of machined specimens confirmed that Sample number 13 ($Ra = 2.649\ \mu\text{m}$) had higher surface defects and an uneven surface than Sample number 2 ($Ra = 1.530\ \mu\text{m}$), which exhibited fewer defects and a finer surface.

12. Surface analysis of the corresponding wire electrodes revealed that less worn-out occurred during machining Sample number 2 compared to Sample number 13.

13. Large craters formed due to a higher pulse-on duration were observed on the surface of the wire electrode used to machine Sample number 13. These large craters could be one reason for the poor surface finish in Sample number 13.

Acknowledgements

The authors thank the Department of Production Technology, Madras Institute of Technology, Chennai, India, for extending its facilities during this study.

References

- [1] C. Veiga, J. P. Davim, A. J. Loureiro, Properties and applications of titanium alloys: A brief review, *Rev. Adv. Mater. Sci.* 32 (2012) 133–148.
- [2] J. D. Majumdar, I. Manna, Laser surface engineering of titanium and its alloys for improved wear, corrosion and high-temperature oxidation resistance. In: J. Lawrence (Ed.), *Laser Surface Engineering*, Elsevier, Woodhead, 2015, pp. 483–521. <https://doi.org/10.1016/C2013-0-16444-6>
- [3] D. Gospodinov, N. Ferdinandov, S. Dimitrov, Classification, properties and application of titanium and its alloys, *Proceedings of University of Ruse* 55 (2016) 27–32.
- [4] A. Pramanik, A. K. Basak, G. Littlefair, S. Debnath, C. Prakash, M. A. Singh, D. Marla, R. K. Singh, Methods and variables in Electrical discharge machining of titanium alloy – A review, *Heliyon* 6 (2020) e05554. <https://doi.org/10.1016/j.heliyon.2020.e05554>
- [5] S. R. Oke, G. S. Ogunwande, M. Onifade, E. Aikulola, E. D. Adewale, O. E. Olawale, B. E. Ayodele, F. Mwema, J. Obiko, An overview of conventional and non-conventional techniques for machining of titanium alloys, *Manufacturing Review* 34 (2020) 1–24. <https://doi.org/10.1051/mfreview/2020029>
- [6] M. Manjaiah, S. Narendranath, S. Basavarajappa, A review on machining of titanium-based alloys using EDM and WEDM, *Rev. Adv. Mater. Sci.* 36 (2014) 89–111.
- [7] B. K. Kumar, V. C. Das, Perspective and prospects of Wire Electric Discharge Machining (WEDM), *Journal of Engineering & Technological Sciences* 54 (2022) 979–998. <https://doi.org/10.5614/j.eng.technol.sci.2022.54.5.9>
- [8] H. R. Basavaraju, S. S. Manjunatha, R. Suresh, Investigation on surface roughness and MRR in WEDM of Titanium Grade 7 (Ti-0.15 Pd) alloy using statistical techniques, *Journal of Mechanical Engineering* 20

- (2023) 73–90.
<https://doi.org/10.24191/jmeche.v20i2.22055>
- [9] K. V. Venkata Nagaraju, M. Joseph Davidson, G. Venkatesh, M. Manjaiah, K. Harikrishna, Optimization of wire-electric discharge machining and metallurgical characteristics of Ti-16Al-14Nb (α/β , ML-Grade) Alloy, *J. of Mater. Eng. and Perform.* (2023).
<https://doi.org/10.1007/s11665-023-08965-4>
- [10] S. Ezeddini, W. Rajhi, M. Boujelbene, E. Bayraktar, S. B. Salem, An investigation to achieve good surface integrity in Wire Electrical Discharge Machining of Ti-6242 super alloy, *J. of Mater. Eng. and Perform.* (2023).
<https://doi.org/10.1007/s11665-023-08270-0>
- [11] E. K. Mussada, Modelling and prediction of WEDM parameters for sustainable machining of titanium grade-2 alloy, *World Journal of Engineering* 21 (2022) 357–367.
<https://doi.org/10.1108/WJE-05-2022-0201>
- [12] K. Satyanarayana, M. Mounika, K. R. Kiran, Experimental studies and optimization of WEDM process in machining of Inconel 600 using zinc wire, *Materials Today: Proceedings* 44 (2021) 2431–2434.
<https://doi.org/10.1016/j.matpr.2020.12.475>
- [13] R. Prasanna, V. Kavimani, P. M. Gopal, D. Simson, Multi-response optimization and surface integrity characteristics of wire electric discharge machining α -phase Ti-6242 alloy, *Process Integration and Optimization for Sustainability* 5 (2021) 815–826.
<https://doi.org/10.1007/s41660-021-00179-2>
- [14] V. Aggarwal, J. Singh, S. Sharma, A. Sharma, G. Singh, J. Parshad, Empirical Modelling of Machining Parameters During WEDM of Inconel 690 Using Response Surface Methodology, *Proceedings of 3rd International Conference On Inventive Material Science Applications, ICIMA03 (2020)*, pp. 1-14. ISBN 978-073-54401-1
- [15] P. Sai Kumar, M. S. R. Niranjan Kumar, P. Gopala Krishnaiah, Optimization of process parameters of wire cut electrical discharge machining on Titanium Grade-5 material using Design of Experiments, *International Journal of Innovative Technology and Exploring Engineering* 8 (2019) 3937–3946.
<https://doi.org/10.35940/ijitee.K1937.0981119>
- [16] H. Majumder, K. P. Maity, Predictive analysis on responses in WEDM of titanium grade 6 using general regression neural network (GRNN) and multiple regression analysis (MRA), *Silicon* 10 (2018) 1763–1776.
<https://doi.org/10.1007/s12633-017-9667-1>
- [17] V. Kumar, K. K. Jangra, V. Kumar, N. Sharma, GA-based optimisation using RSM in WEDM of Nimonic-90: A nickel-based super alloy, *International Journal of Industrial and Systems Engineering* 28 (2018) 53–69.
<https://doi.org/10.1504/IJISE.2018.088564>
- [18] L. W. Reolon, C. A. Henning Laurindo, R. D. Torres, F. L. Amorim, WEDM performance and surface integrity of Inconel alloy IN718 with coated and uncoated wires, *The International Journal of Advanced Manufacturing Technology* 100 (2019) 1981–1991.
<https://doi.org/10.1007/s00170-018-2828-6>
- [19] S. P. Jain, H. V. Ravindra, G. Ugrasen, G. N. Prakash, Y. S. Rammohan, Study of surface roughness and AE signals while machining titanium grade-2 material using ANN in WEDM, *Materials Today: Proceedings* 4 (2017) 9557–9560.
<https://doi.org/10.1016/j.matpr.2017.06.223>
- [20] S. K. Mishra, R. Davis, Experimental investigation in machining of CP Titanium Grade-2 by Wire EDM, *International Journal of Research in Mechanical Engineering & Technology* 6 (2016) 150–153.
- [21] J. B. Saedon, N. Jaafar, N. H. Mohamad Nor, M. A. Yahaya, H. Husain, Multi-objective optimization in wire-electrical discharge machining (WEDM) of titanium alloy, *Jurnal Teknologi* 76 (2015) 31–35.
<https://doi.org/10.11113/jt.v76.5670>
- [22] C. Nandakumar, B. Mohan, Multi-Response Optimization of CNC WEDM process parameters for machining titanium alloy Ti 6Al-4V using Response Surface Methodology (RSM), *Applied Mechanics and Materials* 541 (2014) 354–358.
<https://doi.org/10.4028/www.scientific.net/AMM.541-542.354>
- [23] M. K. Gupta, P. Niesłony, M. Sarikaya, M. E. Korkmaz, M. Kuntoglu, G. M. Krolczyk, M. Jamil, Tool wear patterns and their promoting mechanisms in hybrid cooling assisted machining of titanium Ti-3Al-2.5 V/grade 9 alloy, *Tribology International* 174 (2022) 107773.
<https://doi.org/10.1016/j.triboint.2022.107773>
- [24] S. Ranga, M. Jaimini, S. K. Sharma, B. S. Chauhan, A. Kumar, A review on design of experiments (DOE), *Int. J. Pharm. Chem. Sci.* 3 (2014) 216–224.
- [25] J. Kapoor, S. Singh, J. S. Khamba, High-performance wire electrodes for wire electrical-discharge machining – A review, *Proceedings of the Institution of Mechanical Engineers, Part B: Journal of Engineering Manufacture* 226 (2012) 1757–1773.
<https://doi.org/10.1177/0954405412460354>
- [26] M. K. Das, K. Kumar, T. K. Barman, P. Sahoo, Optimization of WEDM process parameters for MRR and surface roughness using Taguchi-based grey relational analysis, *International Journal of Materials Forming and Machining Processes* 2 (2015) 1–25.
<https://doi.org/10.4018/ijmfmp.2015010101>
- [27] R. Nur, M. Muas, Apollo, S. Risal, Effect of current and wire speed on surface roughness in the manufacturing of straight gear using wire-cut EDM process, *IOP Conf. Series: Materials Science and Engineering* 619 (2019) 012002.
<https://doi.org/10.1088/1757-899X/619/1/012002>
- [28] M. T. Antar, S. L. Soo, D. K. Aspinwall, D. Jones, R. Perez, Productivity and workpiece surface integrity when WEDM aerospace alloys using coated wires, *Procedia Engineering* 19 (2011) 3–8.
<https://doi.org/10.1016/j.proeng.2011.11.071>
- [29] M. S. Priyan, J. D. Darwin, Investigation of surface roughness, kerf width and MRR on AISI D2 steel machined by Wire EDM, *Chemical and Materials Engineering* 5 (2017) 55–64.
<https://doi.org/10.13189/cme.2017.050301>
- [30] M. D. Karim Baig, N. Venkaiah, Parametric optimization of WEDM for Hastelloy C 276 using GRA method, *Int. J. Eng. Dev. Res.* 1 (2014) 1–7.
- [31] M. A. Moghaddam, F. Kolahan, Modeling and optimization of surface roughness of AISI 2312 hot worked steel in EDM based on mathematical modeling and genetic algorithm, *International Journal of Engineering* 27 (2014) 417–424.
<https://doi.org/10.5829/idosi.ije.2014.27.03c.09>
- [32] J. Bérubé, C. F. Wu, Signal-to-noise ratio and related measures in parameter design optimization: An

- overview, The Indian Journal of Statistics Series B 1 (2000) 417–432.
- [33] S. Lal, S. Kumar, Z. A. Khan, A. N. Siddiquee, Multi-response optimization of wire electrical discharge machining process parameters for Al7075/Al₂O₃/SiC hybrid composite using Taguchi-based grey relational analysis, Proceedings of the Institution of Mechanical Engineers, Part B: Journal of Engineering Manufacture 229 (2015) 229–237. <https://doi.org/10.1177/0954405414526382>
- [34] S. Athreya, Y. D. Venkatesh, Application of Taguchi method for optimization of process parameters in improving the surface roughness of lathe facing operation, International Refereed Journal of Engineering and Science 1 (2012) 13–19.
- [35] Y. Nawaz, S. Maqsood, K. Naeem, R. Nawaz, M. Omair, T. Habib, Parametric optimization of material removal rate, surface roughness, and kerf width in high-speed wire electric discharge machining (HS-WEDM) of DC53 die steel, The International Journal of Advanced Manufacturing Technology 107 (2020) 3231–3245. <https://doi.org/10.1007/s00170-020-05175-3>.
- [36] V. Parashar, A. Rehman, J. L. Bhagoria, Y. M. Puri, Kerfs width analysis for wire cut electro discharge machining of SS 304L using design of experiments, Indian Journal of Science and Technology 3 (2010) 369–373. <https://doi.org/10.17485/ijst/2010/v3i4.4>
- [37] R. Abdallah, S. L. Soo, R. Hood, The Influence of cut direction and process parameters in wire electrical discharge machining of carbon fibre-reinforced plastic composites, The International Journal of Advanced Manufacturing Technology 113 (2021) 1699–1716. <https://doi.org/10.1007/s00170-021-06641-2>
- [38] R. M. Kirwin, M. P. Jahan, Effects of non-electrical parameters on profile accuracies and surface characteristics during wire-EDM of titanium alloy, Machining Science and Technology 25 (2021) 1031–1052. <https://doi.org/10.1080/10910344.2021.1971714>.
- [39] A. Pramanik, A. K. Basak, C. Prakash, Understanding the wire electrical discharge machining of Ti-6Al-4V alloy, Heliyon 5 (2019) e01473. <https://doi.org/10.1016/j.heliyon.2019.e01473>
- [40] S. Habib, Optimization of machining parameters and wire vibration in wire electrical discharge machining process, Mechanics of Advanced Materials and Modern Processes 3 (2017) 3. <https://doi.org/10.1186/s40759-017-0017-1>
- [41] D. M. Shivanna, M. B. Kiran, S. D. Kavitha, Evaluation of 3D surface roughness parameters of EDM components using vision system, Procedia Materials Science 5 (2014) 2132–2141. <https://doi.org/10.1016/j.mspro.2014.07.416>
- [42] N. Naeim, M. A. Abou Eleaz, A. Elkaseer, Experimental investigation of surface roughness and material removal rate in Wire EDM of stainless steel 304, Materials 16 (2023) 1022. <https://doi.org/10.3390/ma16031022>
- [43] T. Chaudhary, A. N. Siddiquee, A. K. Chanda, Effect of wire tension on different output responses during wire electric discharge machining on AISI 304 stainless steel, Defence Technology 15 (2019) 541–544. <https://doi.org/10.1016/j.dt.2018.11.003>.
- [44] T. Dereje, S. Palani, M. Desta, R. Čep, Experimental investigation into the influence of the process parameters of Wire Electric Discharge Machining using Nimonic-263 superalloy, Materials 16 (2023) 5440. <https://doi.org/10.3390/ma16155440>
- [45] A. Raj, J. P. Misra, D. Khanduja, K. K. Saxena, V. Malik, Design, modeling and parametric optimization of WEDM of Inconel 690 using RSM-GRA approach, International Journal on Interactive Design and Manufacturing (IJIDeM) 11 (2022) 2107–2117. <https://doi.org/10.1007/s12008-022-00947-5>
- [46] A. Mostafapor, H. Vahedi, Wire electrical discharge machining of AZ91 magnesium alloy: Investigation of effect of process input parameters on performance characteristics, Engineering Research Express 1 (2019) 015005. <https://doi.org/10.1088/2631-8695/ab26c8>.
- [47] K. D. Mohapatra, R. Dash, S. K. Sahoo, Comparative study of wire electrodes in a wire EDM gear cutting process using Grey Moora method, Int. J. Technol. Res. Eng. 6 (2019) 4911–4920.